

Learning a Dilated Residual Network for SAR Image Despeckling

Qiang Zhang, Zhen Yang, Qiangqiang Yuan, *Member, IEEE*, Jie Li, Xiaoshuang Ma, Huanfeng Shen, *Senior Member, IEEE*,
Liangpei Zhang, *Senior Member, IEEE*

Abstract—In this letter, to break the limit of the traditional linear models for SAR image despeckling, we propose a novel deep learning approach by learning a non-linear end-to-end mapping between the noisy and clean SAR images with a dilated residual network (SAR-DRN). SAR-DRN is based on dilated convolutions, which can both enlarge the receptive field and maintain the filter size and layer depth with a lightweight structure. In addition, skip connections are added to the despeckling model to reduce the vanishing gradient problem. Compared with the traditional despeckling methods, the proposed method shows superior performance over the state-of-the-art methods on both quantitative and visual assessments, especially for strong speckle noise.

Index Terms—SAR image despeckling, dilated convolutions, skip connections, residual learning.

I. INTRODUCTION

Synthetic aperture radar (SAR) is a coherent imaging sensor, which can access a wide range of high-quality massive surface data. However, SAR images are inherently affected by multiplicative noise, i.e., speckle noise, which is caused by the coherent nature of the scattering phenomena [1]. The presence of speckle severely affects the quality of SAR images, and greatly reduces the utilization efficiency in SAR image interpretation, retrieval, and other applications [2]. As a result, SAR image speckle reduction is an essential preprocessing step and has become a hot research topic.

To remove the speckle noise of SAR images, researchers first proposed spatial linear filters such as the Lee filter [3]. This method assumes that the image filtering result values have a linear relationship with the original image. However, due to the nature of local processing, the spatial linear filter methods often fail to preserve edges and details.

Aimed at solving this problem, the nonlocal means (NLM) algorithm [4] has provided a breakthrough in detail preservation in SAR image despeckling. The basic idea of the NLM-based methods is that natural images have self-similarity and there are similar patches repeating over and over throughout the whole image. For instance, the SAR-BM3D algorithm [5] uses the local linear minimum mean square error (MMSE) criterion and undecimated wavelet transform. However, the low computational efficiency of the similar patch searching restricts its application.

In addition, the variational methods [6] have gradually been utilized for SAR image despeckling because of their stability and flexibility. The despeckling task is cast as the inverse problem of recovering the original noise-free image based upon reasonable assumptions or prior knowledge of the noise

observation model. Although these variational methods [7]–[8] have achieved good reduction of speckle noise, the result is usually dependent on the choice of the model parameters and prior models.

In general, although a lot of SAR despeckling methods have been proposed, they sometimes fail to preserve sharp features in domains of complicated texture, or even create some block artifacts in the speckled image. In this letter, considering that image speckle noise can be expressed more accurately through non-linear models than linear models, and to overcome the limitations of the linear models, we propose a novel deep neural network based approach for SAR image despeckling, learning a non-linear end-to-end mapping between the speckled and clean SAR images by a dilated residual network (SAR-DRN). Our despeckling model employs dilated convolutions [9] and skip connections with residual learning strategy. Compared with the traditional despeckling methods, the proposed approach shows a state-of-the-art performance in both quantitative and visual assessments, especially for strong speckle noise.

The rest of this letter is organized as follows. The SAR image speckling noise degradation model and the related deep neural network method are introduced in Section II. The network architecture of the proposed method is described in Section III. The results of the despeckling assessment in both simulated and real experiments are presented in Section IV. Finally, the conclusions are summarized in Section V.

II. RELATED WORK

A. SAR Image Speckling Noise Degradation Model

For SAR images, the main reason for the degradation of the image quality is multiplicative speckle noise. Differing from additive white Gaussian noise (AWGN), speckle noise is described by the multiplicative noise model:

$$y = x \cdot n \quad (1)$$

where y is the speckled noise image, x is the clean image, and n represents the speckle noise. It is well-known that, for SAR amplitude image, the speckle follows a Rayleigh distribution [8]:

$$\rho_n(n) = \frac{L^n n^{L-1} \exp(-nL)}{\Gamma(L)} \quad (2)$$

where $L \geq 1$, $n \geq 0$, Γ is the gamma function, and L is the equivalent number of looks (ENL), as defined in (3), which is usually regarded as the quantitative evaluation index for real SAR image despeckling experiments in the homogeneous areas.

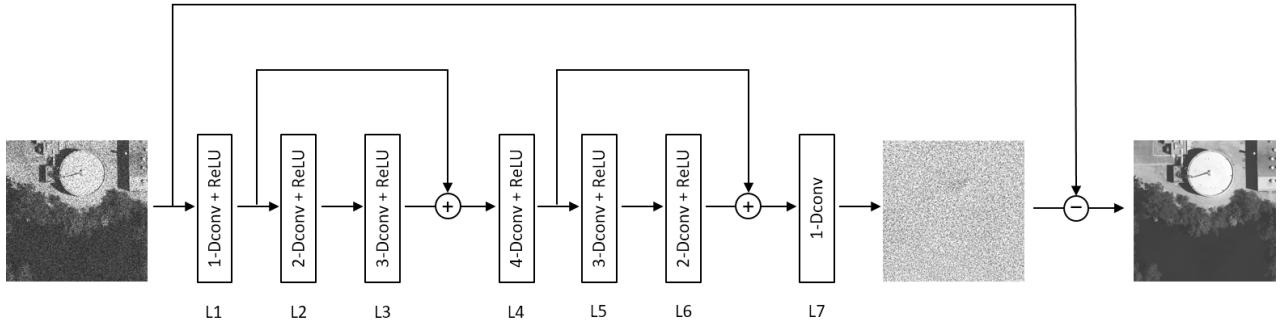


Fig. 2. The architecture of the proposed SAR-DRN.

$$ENL = \frac{mean^2}{std^2} \quad (3)$$

where $mean$ and std respectively represent the image mean and standard deviation.

Therefore, for this non-linear multiplicative noise, choosing a non-linear expression for speckle reduction is an important strategy. In the following, we briefly introduce the use of convolutional neural networks (CNNs) for SAR image despeckling, considering both the low-level features as the bottom level and the output feature representation from the top level of the network.

B. CNNs for SAR Image Despeckling

Recently, benefiting from the powerful non-linear expression of deep convolution neural networks (DCNNs), CNNs have gradually become an efficient image processing method which has been successfully applied to many computer vision tasks such as image classification, segmentation, object recognition, and so on [17]. CNNs can extract the image internal features and avoid the complex preprocessing of images, organized in a feature map of $m_1 \times n_1 \times c_1$, within which each unit is connected to local patches of the previous layer through a set of weight parameters W of size $k_1 \times k_2 \times N$ and bias parameters b . The output feature map is:

$$f^s = \sum_{i=1}^N W_i^s * x^i + b^s \quad (4)$$

where $*$ is a two-dimensional discrete convolution operation, f^s is the output feature map of size $m_2 \times n_2 \times c_2$, and x^i is the i -th input feature map. Specially, the network parameters W and b need to be regenerated through back-propagation and the chain rule of derivation.

To ensure that the output of the CNN is a non-linear combination of the input, a non-linear function is introduced as an excitation function, such as the rectified linear unit (ReLU):

$$z^s = \max(0, f^s) \quad (5)$$

For speckle noise reduction, a new method named the feed-forward SAR despeckling convolutional neural network (SAR-CNN) [10], as shown in Fig. 1, has recently shown excellent performances in contrast with the traditional methods. Along with batch normalization (BN) and a ReLU activation function as [11], and a component-wise division residual layer to estimate the speckled image, SAR-CNN uses the homomorphic approach with coupled logarithm and exponent transforms in combination with a similarity measure

for speckle noise distribution.

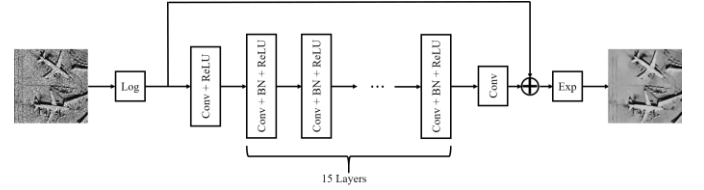


Fig. 1. The architecture of SAR-CNN [10].

III. METHODOLOGY

In this letter, rather than using log transform or modifying the loss function, we propose a novel network, which is trained in an end-to-end fashion using a combination of dilated convolutions and skip connections. Instead of relying on pre-determined image *a priori* knowledge or a noise description model, the main superiority of using the deep neural network strategy for SAR image despeckling is that the model can directly acquire and update the network parameters from the training data and the corresponding labels.

The proposed holistic neural network model for SAR image despeckling contains seven dilated convolution layers and two skip connections, as illustrated in Fig. 2. In addition, the proposed model uses a residual learning strategy to predict the speckled image, which adequately utilizes the non-linear expression ability of deep learning. The details of the algorithm are described in the following.

A. Dilated Convolutions

In image restoration problems such as single-image super-resolution (SISR) and denoising and deblurring, contextual information can effectively facilitate the recovery of degraded regions. In deep convolutional networks, they mainly augment the contextual information through enlarging the receptive field. Generally speaking, there are two ways to achieve this purpose: 1) increasing the network depth; and 2) enlarging the filter size. Nevertheless, as the network depth increases, the accuracy becomes “saturated” and then degrades rapidly. Enlarging the filter size can also lead to more convolution parameters, which greatly increases the calculative burden and training times.

To solve this problem effectively, dilated convolutions were first proposed in [9], which is an approach that can both enlarge the receptive field and maintain the filter size. Setting kernel size=3×3 as an example, Fig. 3 illustrates the dilated convolution receptive field size.

The common convolution receptive field has a linear correlation with the layer depth, in that the receptive field size $F_{depth-i} = (2i + 1) \times (2i + 1)$, while the dilated convolution

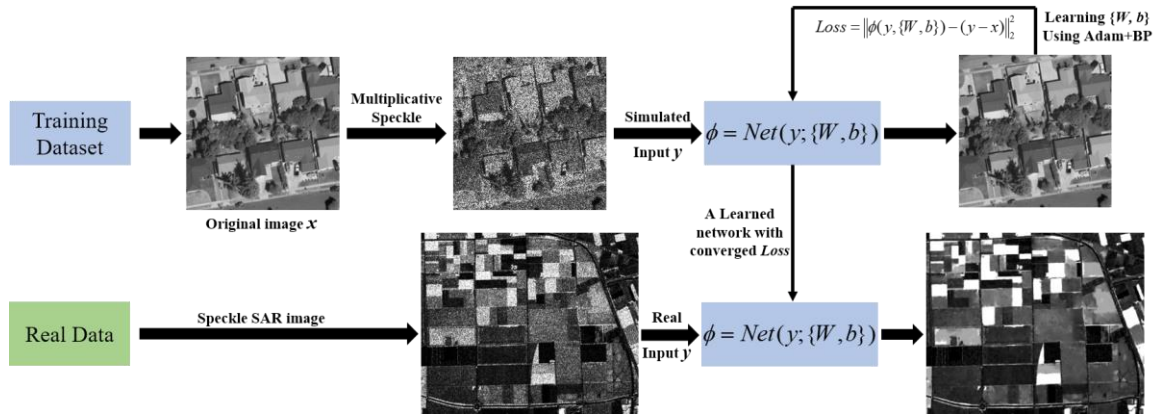


Fig. 4. The framework of SAR image despeckling based on deep learning.

receptive field has an exponential correlation with the layer depth, that $F_{depth-i} = (2^{i+1} - 1) \times (2^{i+1} - 1)$.

In the proposed model, the dilation factors of the 3×3 dilated convolutions from layer 1 to layer 7 are respectively set to 1, 2, 3, 4, 3, 2, and 1. Compared with other deep networks, we propose a lightweight model with only seven dilated convolution layers, as shown in Fig. 2.

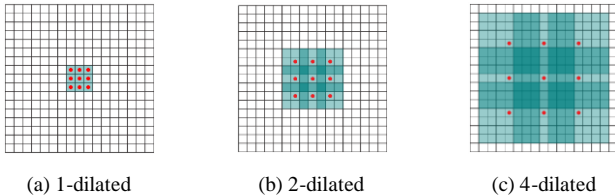


Fig. 3. Dilated convolution receptive field size.

B. Skip Connections

Although the increase of network layer depth can help to obtain more data feature expressions, it often results in the vanishing gradient problem, which makes the training of the model much harder. To solve this problem, a new structure called the skip connection [12] has been created for the DCNNs. The skip connection can pass the previous layer's feature information to its posterior layer, maintaining the image details and avoiding or reducing the vanishing gradient problem. In the proposed model, two skip connections are employed to connect layer 1 to layer 3 (as shown in Fig. 2) and layer 4 to layer 7.

C. Residual Learning

Compared with traditional data mapping, He et al. [12] found that residual mapping can acquire a more effective learning effect and rapidly reduce the loss after passing through a multi-layer network. It is reasonable to consider that most pixel values in residual image are very close to zero, and the spatial distribution of the residual feature maps should be very sparse, which can transfer the gradient descent process to a much smoother hyper-surface of loss to filtering parameters. Thus, searching for an allocation which is on the verge of the optimal for the network's parameters becomes much quicker and easier, allowing us to add more layers to the network and improve its performance.

Specifically, given a collection of N training image pairs $\{x_i, y_i\}_N$, y_i is the speckled image, x_i is the clean image,

and Θ is the network parameters. Our model uses the mean squared error (MSE) as the loss function:

$$loss(\Theta) = \frac{1}{2N} \sum_{i=1}^N \|\phi(y_i, \Theta) - (y_i - x_i)\|_2^2 \quad (6)$$

In summary, with the dilated convolutions and skip connections structure, the flowchart of learning a deep network for the SAR image despeckling process is described in Fig. 4.

IV. EXPERIMENTS AND DISCUSSIONS

A. Implementation Details

1) Training and Test Datasets: In this paper, the amplitude images are processed by the comparison methods and the proposed method. For SAR image despeckling with different numbers of looks, we used the UC Merced land-use dataset [13] as our training dataset. To train the proposed SAR-DRN, we chose 400 images of size 256×256 from this dataset and set each patch size as 40×40 and stride=10. To test the performance of the proposed model, single examples of the Airplanes and Buildings classes were respectively set up as simulated images. For the real SAR image despeckling, we used the classic Flevoland SAR image (cropped to 500×600), which is commonly used in real SAR data image despeckling.

2) Parameter Setting and Network Training: Table I lists the parameters of each layer for SAR-DRN. The proposed model was trained using the Adam [14] algorithm as the gradient descent optimization method where the learning rate was initialized to 0.01 for the whole network. The training process of SAR-DRN took 50 epochs, which uses Caffe [15] to train the proposed SAR-DRN in the Windows 7 environment, with an Intel Xeon E5-2609 v3 CPU at 1.90 GHz and an Nvidia Titan-X (Pascal) GPU.

TABLE I. THE NETWORK CONFIGURATION.

	Configurations
Layer 1	Dilated Conv + ReLU: $1 \times 64 \times 3 \times 3$, dilate=1, pad=1
Layer 2	Dilated Conv + ReLU: $1 \times 64 \times 3 \times 3$, dilate=2, pad=2
Layer 3	Dilated Conv + ReLU: $1 \times 64 \times 3 \times 3$, dilate=3, pad=3
Layer 4	Dilated Conv + ReLU: $1 \times 64 \times 3 \times 3$, dilate=4, pad=4
Layer 5	Dilated Conv + ReLU: $1 \times 64 \times 3 \times 3$, dilate=3, pad=3
Layer 6	Dilated Conv + ReLU: $1 \times 64 \times 3 \times 3$, dilate=2, pad=2
Layer 7	Dilated Conv: $1 \times 64 \times 3 \times 3$, dilate=1, pad=1

Table II. PSNR (dB) AND SSIM RESULTS FOR AIRPLANE AND BUILDING.

Looks	Airplane				Building			
	$L=1$	$L=2$	$L=4$	$L=8$	$L=1$	$L=2$	$L=4$	$L=8$
Noisy	10.21/0.2249	12.98/0.3016	15.91/0.3926	18.92/0.4962	13.96/0.2312	16.66/0.3386	19.66/0.5692	22.55/0.5960
PPB	20.01/0.5159	21.74/0.5972	23.49/0.6786	25.01/0.7424	25.06/0.7179	26.34/0.7809	28.05/0.8358	29.49/0.8706
SAR-BM3D	<u>21.88/0.6242</u>	<u>23.65/0.6964</u>	<u>25.49/0.7566</u>	<u>27.15/0.8023</u>	<u>26.18/0.7888</u>	<u>27.96/0.8352</u>	<u>29.87/0.8807</u>	31.37/0.9049
SAR-POTDF	21.73/0.6062	<u>23.98/0.6857</u>	<u>25.86/0.7513</u>	<u>27.57/0.7940</u>	24.81/0.7284	27.40/0.8121	29.55/0.8640	<u>31.56/0.9013</u>
SAR-CNN	21.63/0.5831	23.63/0.6807	25.78/0.7486	27.09/0.7822	25.18/0.7067	27.14/0.7804	29.36/0.8492	30.85/0.8749
Proposed	22.97/0.6579	24.54/0.7279	26.52/0.7636	28.01/0.8203	26.80/0.7974	28.39/0.8381	30.14/0.8712	32.03/0.9022

B. Simulated-Data Experiments

To verify the effectiveness of the proposed model, four speckle noise levels of $L=1, 2, 4,$ and 8 were set up for the two simulated images. The PSNR and SSIM results of the simulated experiments with the two images are listed in Table II where the best performance is marked in bold and the second-best performance is underlined.

As shown in Table II, the proposed SAR-DRN model obtains all the best PSNR results in the four noise levels. When $L=1$, the proposed method outperforms SAR-BM3D by about 1.1 dB and 0.6 dB for Airplane and Building, respectively. When $L=2$ and 4, SAR-DRN outperforms PPB [4], SAR-POTDF [5], SAR-BM3D [8], and SAR-CNN [10] by at least 0.5 dB/0.7 dB and 0.4 dB/0.3 dB for Airplane/Building, respectively. Compared with the traditional despeckling methods above, the proposed method shows superior performance over the state-of-the-art methods on both quantitative and visual assessments, especially for strong speckle noise.

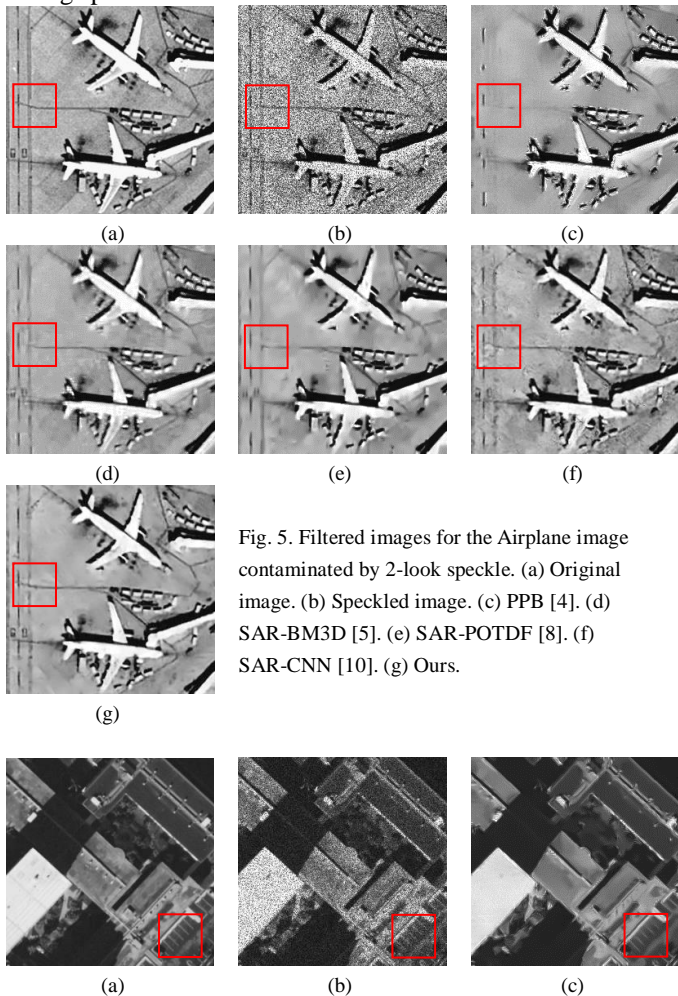


Fig. 5. Filtered images for the Airplane image contaminated by 2-look speckle. (a) Original image. (b) Speckled image. (c) PPB [4]. (d) SAR-BM3D [5]. (e) SAR-POTDF [8]. (f) SAR-CNN [10]. (g) Ours.

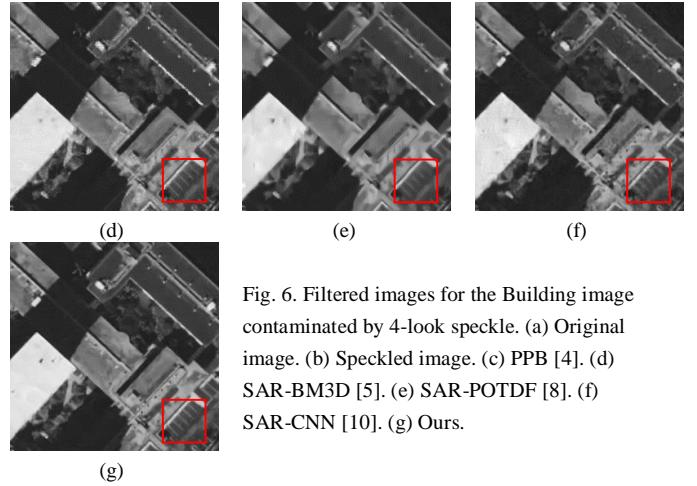


Fig. 6. Filtered images for the Building image contaminated by 4-look speckle. (a) Original image. (b) Speckled image. (c) PPB [4]. (d) SAR-BM3D [5]. (e) SAR-POTDF [8]. (f) SAR-CNN [10]. (g) Ours.

Fig. 5 and Fig. 6 correspondingly show the filtered images for the Airplane and Building images contaminated by 2-look speckle and 4-look speckle, respectively. Compared with the other algorithms above, SAR-DRN achieves the best performance in speckle reduction, concurrently avoiding introducing radiation and geometric distortion. In addition, from the red boxes of the Airplane and Building images in Figs. 5 and 6, respectively, it can be clearly seen that SAR-DRN also shows the best local detail preservation ability, while the other methods either miss partial texture details or produce blurry results, to some extent.

C. Real-Data Experiments

As shown in Fig. 7, we also compared the proposed method with the four state-of-the-art methods described above on a real SAR image. Visually, SAR-DRN achieves the best performance in speckle reduction and local detail preservation, performing better than the other mainstream methods.

In addition, we also evaluated the filtered results through ENL to measure the speckle-reduction ability. The ENL values were estimated from two chosen homogeneous regions (the red boxes in Fig. 8(a)) and are listed in Table III. Clearly, SAR-DRN has a much better speckle-reduction ability than the other methods, which is consistent with the visual observation.

TABLE III. ENL RESULTS FOR THE FLEVLAND IMAGE

Methods	Region I	Region II
PPB	155.2469	125.3481
SAR-BM3D	97.4346	163.2657
SAR-POTDF	140.3258	154.9074
SAR-CNN	118.2997	186.3829
Ours	171.6375	234.8743

D. Discussion

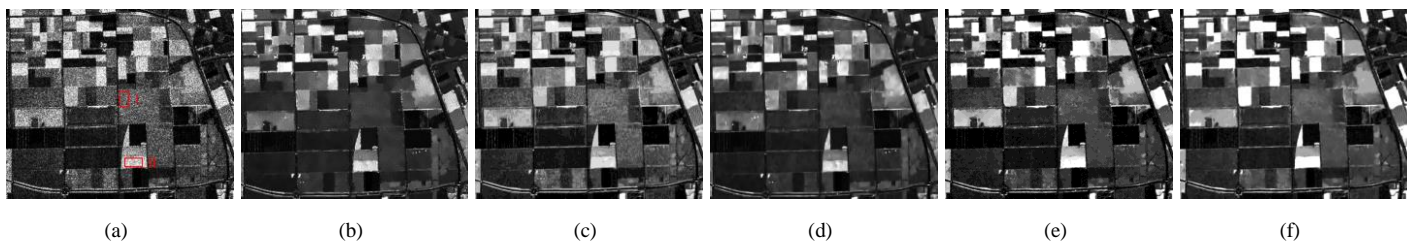


Fig. 7. Filtered images for the Real SAR image contaminated by 4-look speckle. (a) Original image. (b) PPB [4]. (c) SAR-BM3D [5]. (d) SAR-POTDF [8]. (e) SAR-CNN [10]. (f) SAR-DRN.

Dilated Convolutions and Skip Connections: To verify the effectiveness of the dilated convolutions and skip connections, we implemented four sets of experiments in the same environment. As Fig. 8 implies, the dilated convolutions can effectively reduce the training loss and enhance the despeckling performance (PSNR). Meanwhile, the skip connections also accelerate the convergence speed of the network and enhance the model stability.

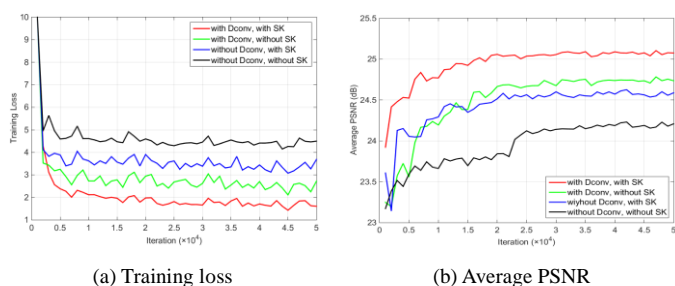


Fig. 8. The simulated SAR image despeckling results of the four specific models in (a) training loss and (b) average PSNR, with respect to iterations. The four specific models were different combinations of dilated convolutions (Dconv) and skip connections (SK), and were trained with 1-look images in the same environment. The results were evaluated on the *Set14* [16] dataset.

V. CONCLUSION

In this letter, we have proposed a novel deep learning approach for the SAR image despeckling task, learning an end-to-end mapping between the noisy and clean SAR images. The presented approach is based on dilated convolutions, which can both enlarge the receptive field and maintain the filter size with a lightweight structure. Furthermore, skip connections are added to the despeckling model to avoid the vanishing gradient problem. Compared with the traditional despeckling methods, the proposed SAR-DRN approach shows a state-of-the-art performance in both simulated and real experiments, especially for strong speckle noise.

In our future work, we will investigate more powerful learning models to deal with the complex real scenes in SAR images. Furthermore, the proposed approach will be extended to polarimetric SAR image despeckling, whose noise model is much more complicated than that of single-polarization SAR.

REFERENCES

- [1] J. W. Goodman, "Some fundamental properties of speckle," *J. Opt. Soc. Am.*, vol. 66, no. 11, pp. 1145–1150, 1976.
- [2] H. Liu, S. Yang, S. Gou, P. Chen, Y. Wang, and L. Jiao, "Fast Classification for Large Polarimetric SAR Data Based on Refined Spatial-Anchor Graph," *IEEE Geosci. Remote Sens. Lett.*, 2017.
- [3] J.-S. Lee, "Digital image enhancement and noise filtering by use of local statistics," *IEEE Trans. Pattern Anal. Mach. Intell.*, no. 2, pp. 165–168, 1980.
- [4] C. A. Deledalle, L. Denis, and F. Tupin, "Iterative weighted maximum likelihood denoising with probabilistic patch-based weights," *IEEE Trans. Image Process.*, vol. 18, no. 12, p. 2661, 2009.
- [5] S. Parrilli, M. Poderico, C. V. Angelino, and L. Verdoliva, "A nonlocal SAR image denoising algorithm based on LMMSE wavelet shrinkage," *IEEE Trans. Geosci. Remote Sens.*, vol. 50, no. 2, pp. 606–616, 2012.
- [6] X. Ma, H. Shen, X. Zhao, and L. Zhang, "SAR image despeckling by the use of variational methods with adaptive nonlocal functionals," *IEEE Trans. Geosci. Remote Sens.*, vol. 54, no. 6, pp. 3421–3435, 2016.
- [7] Feng, W., Lei, H., Gao, Y., "Speckle reduction via higher order total variation approach," *IEEE Trans. Image Process.*, vol. 23, no. 4, pp. 1831–1843, 2014.
- [8] B. Xu *et al.*, "Patch ordering-based SAR image despeckling via transform-domain filtering," *IEEE J. Sel. Topics Appl. Earth Observ. Remote Sens.*, vol. 8, no. 4, pp. 1682–1695, 2015.
- [9] F. Yu and V. Koltun, "Multi-scale context aggregation by dilated convolutions," *arXiv preprint arXiv:1511.07122*, 2015.
- [10] G. Chierchia, D. Cozzolino, G. Poggi, and L. Verdoliva, "SAR image despeckling through convolutional neural networks," *arXiv preprint arXiv:1704.00275*, 2017.
- [11] K. Zhang, W. Zuo, Y. Chen, D. Meng, and L. Zhang, "Beyond a gaussian denoiser: Residual learning of deep CNN for image denoising," *IEEE Trans. Image Process.*, 2017.
- [12] K. He, X. Zhang, S. Ren, and J. Sun, "Deep residual learning for image recognition," in *Proc. IEEE Conf. Computer Vision and Pattern Recognition*, 2016, pp. 770–778.
- [13] Y. Yang and S. Newsam, "Bag-of-visual-words and spatial extensions for land-use classification," in *Proc. 18th SIGSPATIAL Int. Conf. Advances in Geographic Information Systems*, 2010, pp. 270–279.
- [14] D. Kingma and J. Ba, "Adam: A method for stochastic optimization," *arXiv preprint arXiv:1412.6980*, 2014.
- [15] Y. Jia *et al.*, "Caffe: Convolutional architecture for fast feature embedding," in *Proc. 22nd ACM Int. Conf. Multimedia*, 2014, pp. 675–678.
- [16] R. Zeyde, M. Elad, and M. Protter, "On Single Image Scale-Up Using Sparse-Representations," in *Int. Conf. on Curves and Surfaces*, 2010, pp. 711–730.
- [17] L. Zhang, L. Zhang, and B. Du, "Deep Learning for Remote Sensing Data: A Technical Tutorial on the State of the Art," *IEEE Geoscience and Remote Sensing Magazine*, vol. 4, no. 2, pp. 22–40, 2016.